Supporting Information for

Unveiling the role of cobalt in the product regulation for CO_2 hydrogenation to light olefins over alumina-supported Co-Fe catalysts

Zhihao Liu,[a,†] Wenlong Song,[b,†] Peipei Zhang,[c] Jiaming Liang,*[a] Chengwei Wang,[a] Chufeng Liu,[a] Hanyao Song,[a] Baojian Chen,[a] Kangzhou Wang,*[d] Guangbo Liu,[e] Xiaoyu Guo,[a] Yingluo He,[a] Xinhua Gao,[b] Jianli Zhang,[b] Guohui Yang,[a] and Noritatsu Tsubaki*[a]

[a] Department of Applied Chemistry, School of Engineering, University of Toyama, Gofuku 3190, Toyama 930-8555, Japan

[b] State Key Laboratory of High-efficiency Coal Utilization and Green Chemical Engineering, College of Chemistry and Chemical Engineering, Ningxia University, Yinchuan 750021, Ningxia, China

[c] CNOOC Institute of Chemical & Advanced Materials, Beijing 102209, China

[d] School of Materials and New Energy, Ningxia University, Yinchuan 750021, Ningxia, China

[e] Key laboratory of Biofuels, Qingdao Institute of Bioenergy and Bioprocess Technology, Chinese Academy of Sciences, Qingdao 266101, China

Corresponding authors: jmliang@eng.u-toyama.ac.jp (J. Liang), kangzhou_wang@nxu.edu.cn (K. Wang), tsubaki@eng.u-toyama.ac.jp (N. Tsubaki)

† These authors contributed equally.

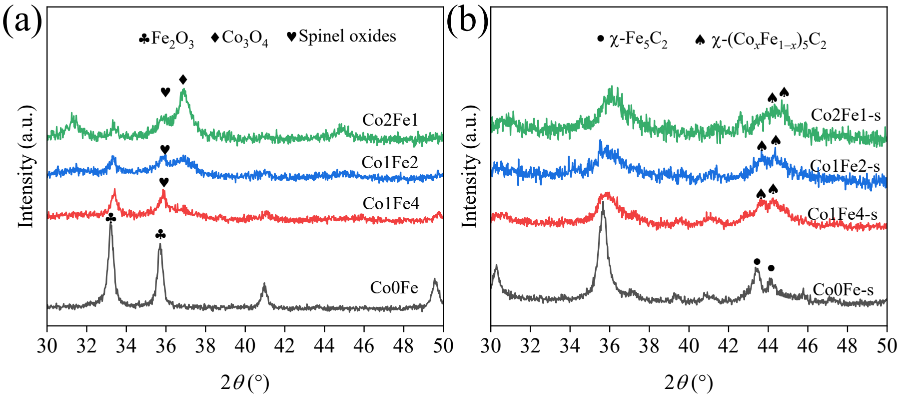

Fig. S1. XRD patterns of (a) the prepared catalysts and (b) spent catalysts within $2\theta =$ 30°–50°.

Table S1

The catalytic performance of state-of-the-art Fe-based catalysts for CO_2 hydrogenation

Catalysts	T (°C)	p (MPa)	CO_2/H_2/ Others	CO_2 conv. (%)	CO and CH_4 sel. (%)	C_2–$C_4^=$ sel. (%)	Yield of C_2–$C_4^=$ (%)	STY of C_2–$C_4^=$ ($g\cdot kg_{cat}^{-1}\cdot h^{-1}$)	Refs.
FeMn	340	2	24/72/4	35.0	28.8	28.2	9.9	165.0	[S1]
$CuFeO_2$	300	1	3 [a]	18.1	35.8	31.3	3.9	-	[S2]
Fe/ZrO_2	320	1.5	14/43/43	38.8	50.0	42.8	13.3	108.1	[S3]
ZnCoFe	320	2.5	24/72/4	49.6	39.2	33.8	15.5	103.4	[S4]
Fe-Co-Mg	320	3	21/63/16	40.6	27.6	36.4	14.8	129.7	[S5]
$CoFeZrO_2$	340	2	24/71/5	40.4	50.0	38.0	12.1	64.2	[S6]
$CoFe_2O_4$/CNT	340	1	23/69/8	34.4	33.4	38.8	10.9	52.2	[S7]
FeCo@C	320	3	21/64/15	52.0	28.5	33.0	17.2	376.6	[S8]
FeCo@ZrO_2	340	3	23/69/8	44.6	42.5	45.0	16.1	236.7	[S9]
Fe-Co-Ni	320	1	3 [a]	47.5	24.3	46.7	22.2	-	[S10]
Co1Fe2	**320**	**3**	**27/68/5**	**51.9**	**21.4**	**44.3**	**22.4**	**315.1**	**This work**

[a] The H_2/CO_2 ratio.

Table S2

The catalytic performance of the prepared catalysts with varying Co/Fe ratios.

Catalysts	CO_2 conv. (%)	CO sel. (%)	CH_4 sel. (%)	C_2–$C_4^=$ sel. (%)	C_2–C_4^o sel. (%)	C_{5+} sel. (%)	STY of C_2–$C_4^=$ ($g \cdot kg_{cat}^{-1} \cdot h^{-1}$)
Co0Fe	36.8	10.3	10.1	35	4.5	50.4	163.0
Co1Fe4	43.6	6.4	18.5	39.2	8.2	34.1	225.7
Co1Fe2	51.9	2.7	18.7	44.3	5.9	31.1	315.1
Co2Fe1	61.6	0.7	42.3	7.7	24.8	25.2	36.1

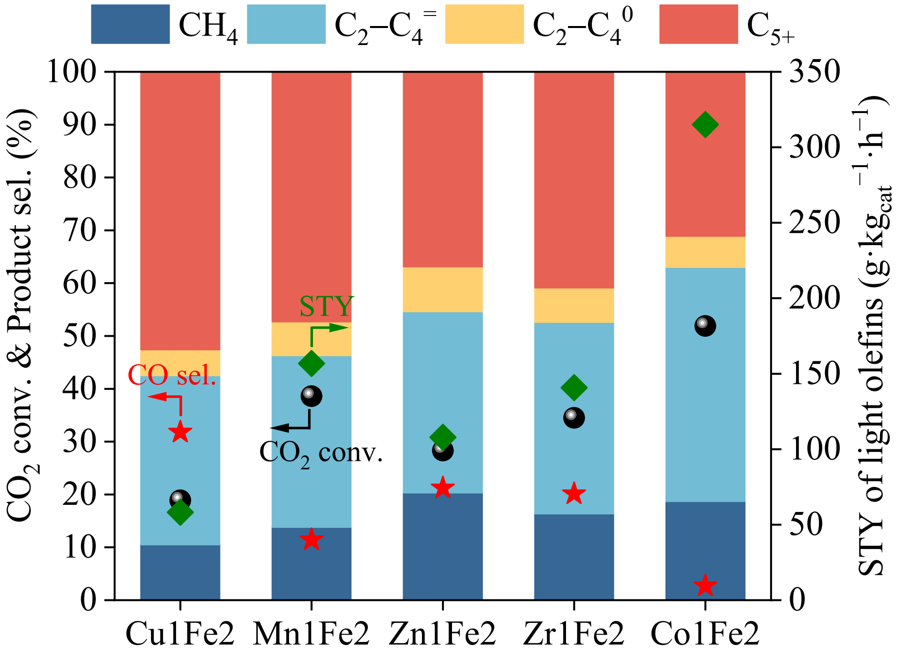

Fig. S2. The catalytic performance of Fe-based catalysts doped with typical metals.

(Reaction conditions: 320 °C, 3 MPa, 9000 mL·g$_{cat}$$^{-1}$·h^{-1}, TOS = 8 h).

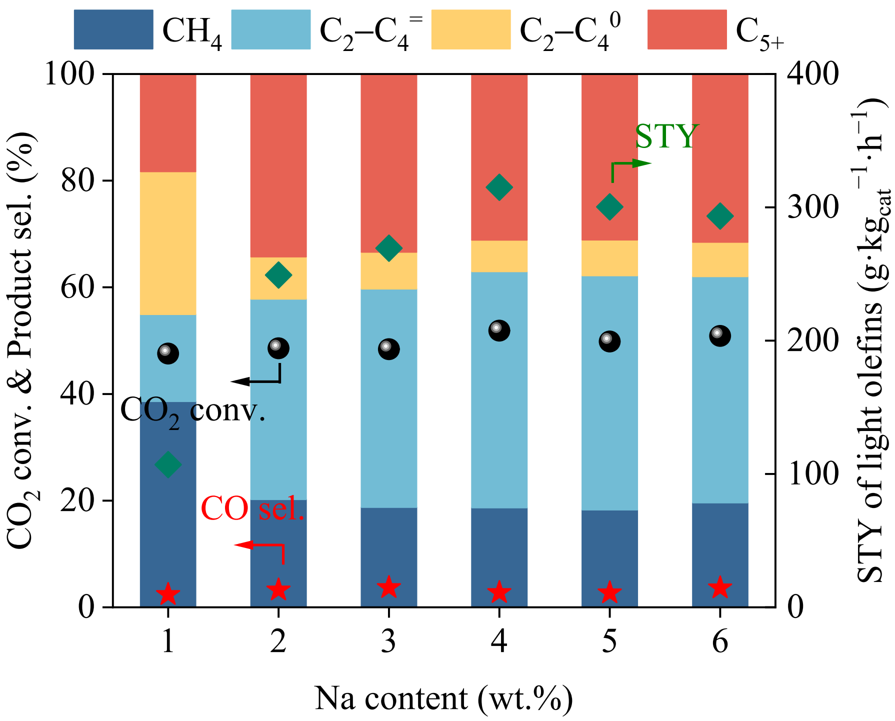

Fig. S3. The effect of Na content on the catalytic performance of Co1Fe2. (Reaction conditions: 320 °C, 3 MPa, 9000 mL·g$_{cat}$$^{-1}$·h^{-1}, TOS = 8 h).

Table S3

Effects of reaction conditions on the catalytic performance of Co1Fe2.

T (ºC)	p (MPa)	GHSV (mL·h^{-1}·g$_{cat}^{-1}$)	CO_2 conv. (%)	CO sel. (%)	CH_4 sel. (%)	C_2−$C_4^{=}$ sel. (%)	C_2−C_4^{o} sel. (%)	C_{5+} sel. (%)	STY of C_2−$C_4^{=}$ (g·kg$_{cat}^{-1}$·h^{-1})
280	3.0	9000	31.6	4.3	27.4	35.7	13.7	23.2	152.3
300	3.0	9000	44.6	4.4	22.2	38.0	8.4	31.4	228.4
320	3.0	9000	51.9	2.7	18.7	44.3	5.9	31.1	315.1
340	3.0	9000	52.1	4.6	18.0	40.4	5.6	36.0	272.3
360	3.0	9000	54.0	6.0	19.5	41.3	6.5	32.7	295.7
380	3.0	9000	54.9	7.5	27.9	35.2	5.6	31.3	252.5
320	2.0	9000	44.0	3.9	17.8	42.5	6.6	33.1	253.4
320	2.5	9000	44.3	2.7	17.7	43.3	7.0	32.1	262.7
320	3.5	9000	53.9	1.9	20.0	43.4	7.9	28.9	297.1
320	3.0	6000	52.5	5.4	16.8	40.2	6.5	36.5	187.8
320	3.0	12000	39.4	7.0	17.5	42.6	7.1	33.1	291.2

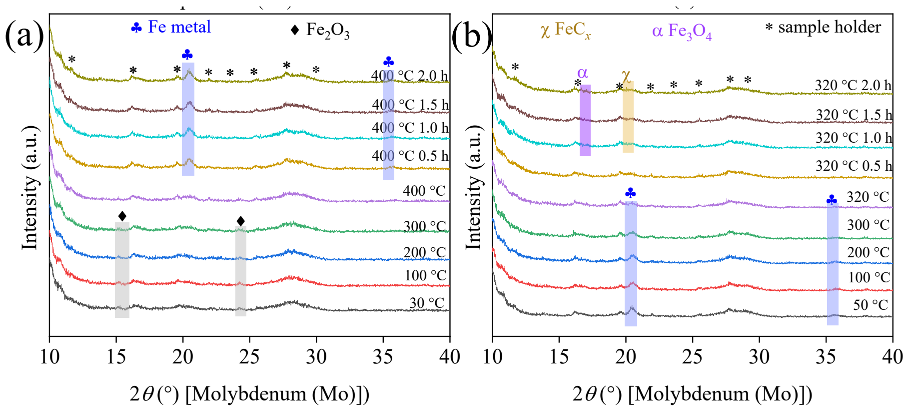

Fig. S4. *In situ* XRD patterns for Co0Fe catalyst during the (a) reduction and (b) reaction process.

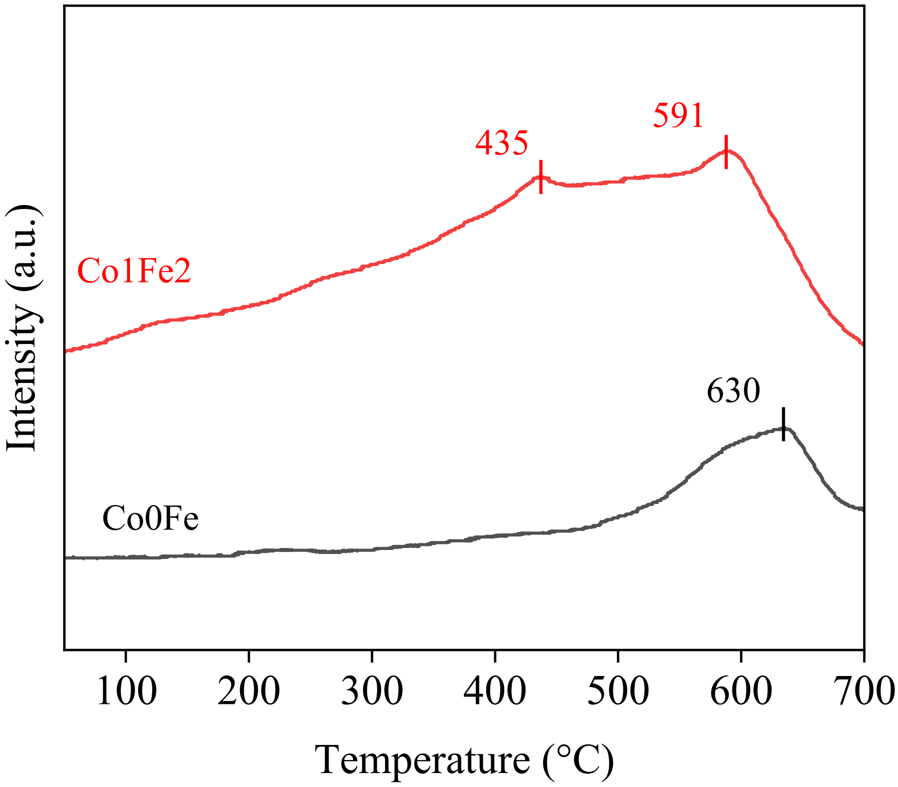

Fig. S5. CO-TPD profiles of the prepared catalysts.

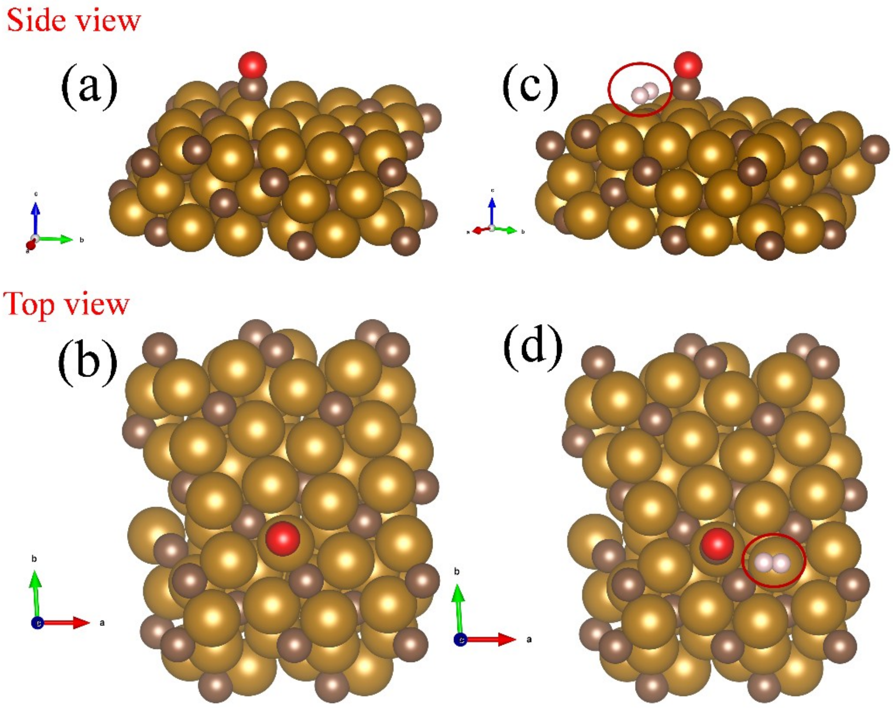

Fig. S6. Side and top views of the Fe$_5$C$_2$ (511) surface with (a,b) pre-adsorbed CO and (c,d) adsorbed CO and H$_2$. Gray, C atoms; Red, O atoms; Light gray, H atoms; Yellow, Fe atoms.

Density functional theory (DFT) calculations. Density functional theory (DFT) calculations were conducted using the Vienna ab initio simulation package (VASP) [S11]. The Perdew-Burke-Ernzerhof (PBE) functional with the generalized gradient approximation was used to describe the electronic exchange and correlation [S12]. The projector augmented-wave (PAW) method was used to treat the interaction between the valence electrons and ionic cores [S13]. K-points were set at 2 × 2 × 1 on a Monkhorst-Pack grid, and a cut-off energy of 500 eV was employed. Gaussian smearing scheme with a small SIGMA of 0.05 was employed. All DFT calculations were performed with the goal of minimizing residual forces until the convergence criterion of 0.02 eV/Å was reached. For vdW-dispersion energy-correction, the DFT-D3 method proposed by Grimme et al. [S14] was utilized.

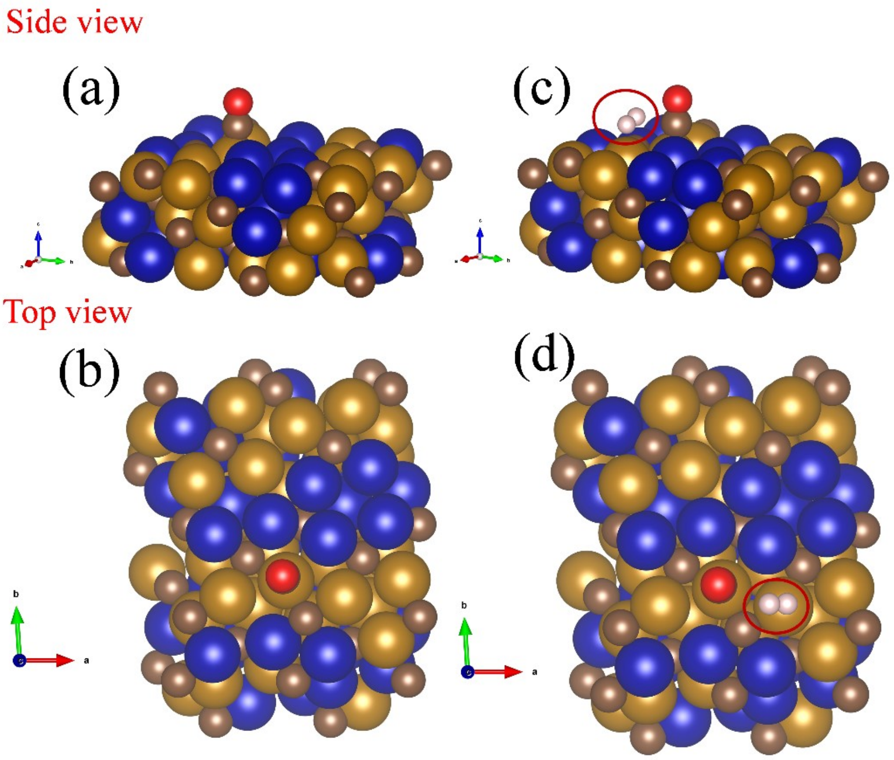

Fig. S7. Side and top views of the $(Co_xFe_{1-x})_5C_2$ (511) surface with (a,b) pre-adsorbed CO and (c,d) adsorbed CO and H_2. Gray, C atoms; Red, O atoms; Light gray, H atoms; Yellow, Fe atoms; Blue, Co atoms.

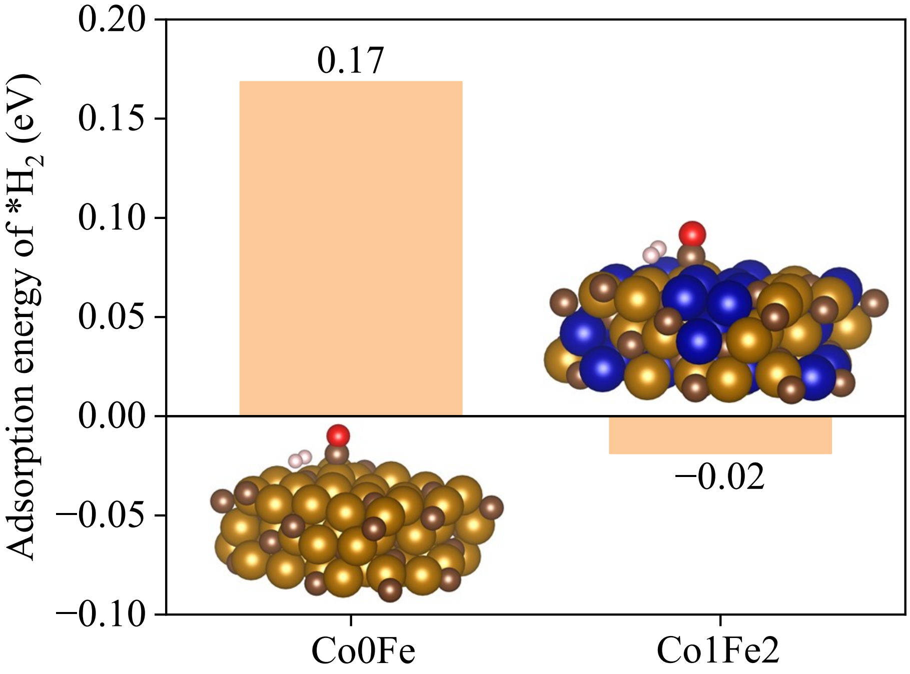

Fig. S8. Adsorption energy of $*H_2$ on the catalyst surface.

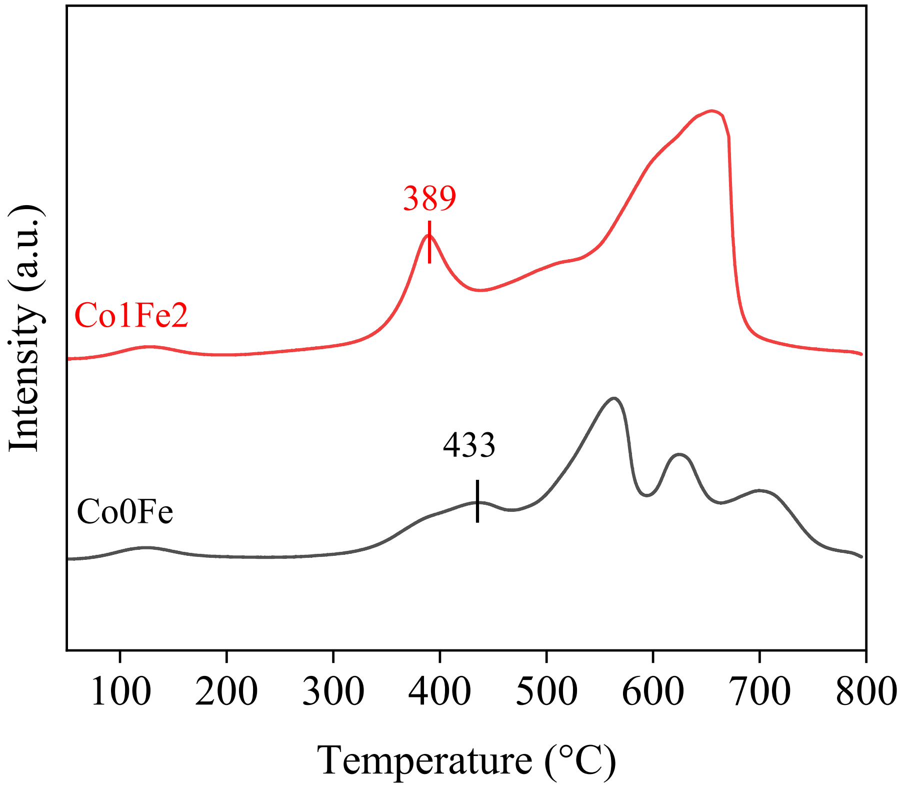

Fig. S9. C_3H_6-TPD profiles of the spent catalysts.

References:

[S1] Y. Xu, P. Zhai, Y. Deng, J. Xie, X. Liu, S. Wang and D. Ma, *Angew. Chem. Int. Ed.*, 2020, **132**, 21920–21928.

[S2] Y.H. Choi, Y.J. Jang, H. Park, W.Y. Kim, Y.H. Lee, S.H. Choi and J.S. Lee, *Appl. Catal. B-Environ.*, 2017, **202**, 605–610.

[S3] J. Huang, S. Jiang, M. Wang, X. Wang, J. Gao and C. Song, *ACS Sustainable Chem. Eng.*, 2021, **9,** 7891–7903.

[S4] Q. Xu, X. Xu, G. Fan, L. Yang and F. Li, *J. Catal.*, 2021, **400**, 355–366.

[S5] F. Yuan, G. Zhang, M. Wang, J. Zhu, M. Zhang, F. Ding, Z. Cheng, C. Song and X. Guo, *Ind. Eng. Chem. Res.*, 2023, **26**, 8210–8221.

[S6] H. Raghav, C. Pendem, S. Tripathi, S. Kumar and B. Sarkar, *Fuel*, 2024, **368**, 131645.

[S7] K.Y. Kim, H. Lee, W.Y. Noh, J. Shin, S.J. Han, S.K. Kim, K. An and J.S. Lee, *ACS Catal.*, 2020, **10**, 8660–8671.

[S8] M. Zhang, L. Zhang, M. Wang, G. Zhang, C. Song and X. Guo, *Chinese J. Catal.*, 2025, **68**, 366–375.

[S9] F. Xu, D. Yang, D. Jin, X. Meng, R. Zhao, W. Dai and Z. Xin, *Ind. Eng. Chem. Res.*, 2024, **63**, 20800–20811.

[S10] Y. Zhao, J. Ma, J. Yin, H. Han, X. Zhang, Y. Cao and W. Cai, *Appl. Surf. Sci.*, 2024, **657**, 159783.

[S11] G. Kresse and J. Furthmüller, *Comput. Mater. Sci.*, 1996, **6**, 15–50.

[S12] J. P. Perdew, K. Burke and M. Ernzerhof, *Phys. Rev. Lett.*, 1996, **77**, 3865.

[S13] P. Blöchl, *Phys. Rev. B*, 1994, **50**, 17953.

[S14] S. Grimme, J. Antony, S. Ehrlich and S. Krieg, *J. Chem. Phys.*, 2010, **132**, 154104.